XXXVIII
International School of Hydraulics
21 - 24 May 2019 • Łąck • Poland

Hydrodynamics of water-worked and screeded gravel-bed flows

Ellora Padhi[1], Nadia Penna[2], Subhasish Dey[1] and Roberto Gaudio[2]

[1] Department of Civil Engineering
Indian Institute of Technology Kharagpur
India

[2] Dipartimento di Ingegneria Civile
Università della Calabria
Italy

Introduction

Flow over a gravel bed is a topic of interest due to its complex three dimensional structure in the near-bed flow region

Resolving the degree of flow spatial heterogeneity is important for estimating flow resistance and performing bedload transport prediction in mountainous rivers

Fig. 1 Photograph of a natural gravel-bed stream

To resolve the spatial heterogeneity, the area averaging is performed over the time-averaged quantity over layer parallel to the mean bed surface, called the *double averaging methodology* (DAM)

In DAM the local instantaneous quantity follows the traditional Reynolds decomposition

$$\theta = \bar{\theta} + \theta'$$

and the local time-averaged quantity is decomposed as

$$\bar{\theta} = \langle \bar{\theta} \rangle + \tilde{\theta}$$

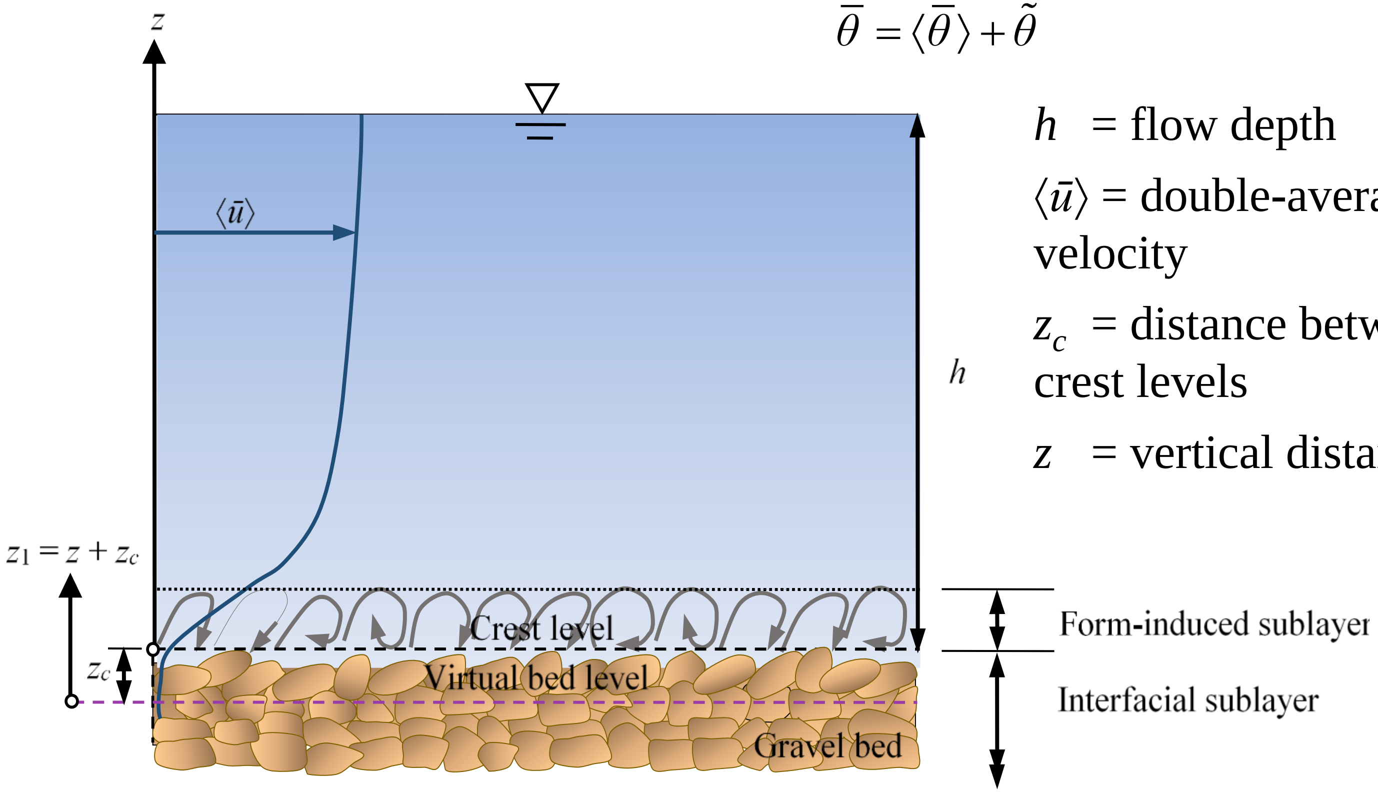

Fig. 2 Schematic of a gravel bed flow.

h = flow depth

$\langle \bar{u} \rangle$ = double-averaged (DA) streamwise velocity

z_c = distance between virtual bed and crest levels

z = vertical distance

Objective

Fig. 3 Photograph of a natural gravel-bed stream (WGB) and a screeded gravel bed (SGB) in a laboratory flume

To examine the DA streamwise velocity and SA turbulent flow parameters in a WGB with respect to an SGB keeping the flow conditions identical in both the beds.

Experimental setup

Experiments were performed in a rectangular flume of 9.6 m long, 0.485 m wide and 0.5 m high at Università della Calabria, Italy

Properties of sediment

Median diameter d_{50} = 4.81 mm

Geometric standard deviation σ_g = 1.18 < 1.4

Hydraulic parameters

Flow Depth h = 0.1 m

Discharge Q = 20 l s^{-1}

Average flow velocity U_{avg} = 0.43 m s^{-1}

Flow Froude number Fr = 0.43

Reynolds number R = 1.12×10^5

Bed slope S_0 = 0.004 and 0.007 for WGB and SGB, respectively

Shear Reynolds number R_* = 80 and 85 for WGB and SGB, respectively

Roughness height K_s = 1.25 mm and 1.04 mm for WGB and SGB, respectively

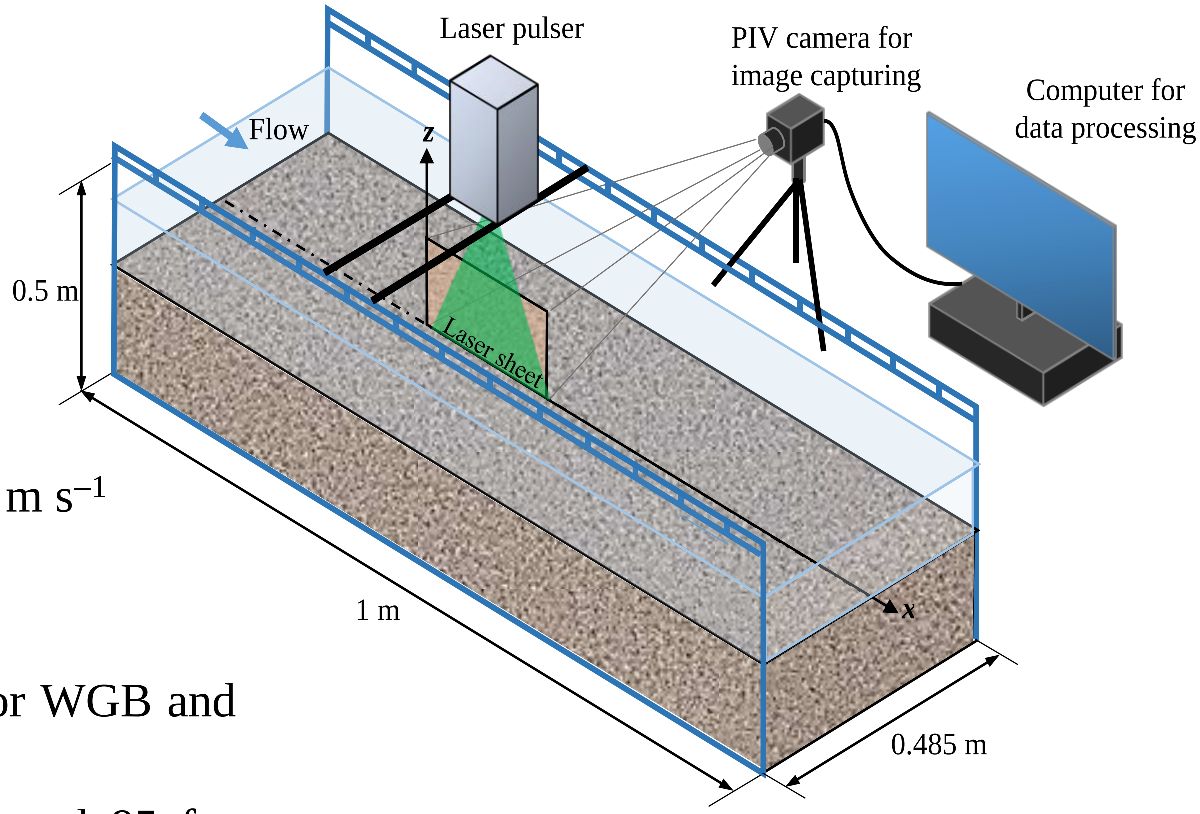

Fig. 4 Schematic of the flume test section showing the flow measuring devices

Results and discussion

Time-averaged velocity vectors and vorticity contours

Time-averaged velocity vectors are expressed as

$$\text{Magnitude} = (\bar{u}^2 + \bar{w}^2)^{0.5}$$

$$\text{Direction} = \tan^{-1}(\bar{w} / \bar{u})$$

where $\bar{u}$ and $\bar{w}$ is the time-averaged streamwise and vertical velocities, respectively

Time-averaged vorticity $\bar{\omega}$ is expressed as

$$\bar{\omega} = \left(\frac{\partial \bar{u}}{\partial z} - \frac{\partial \bar{w}}{\partial x} \right)$$

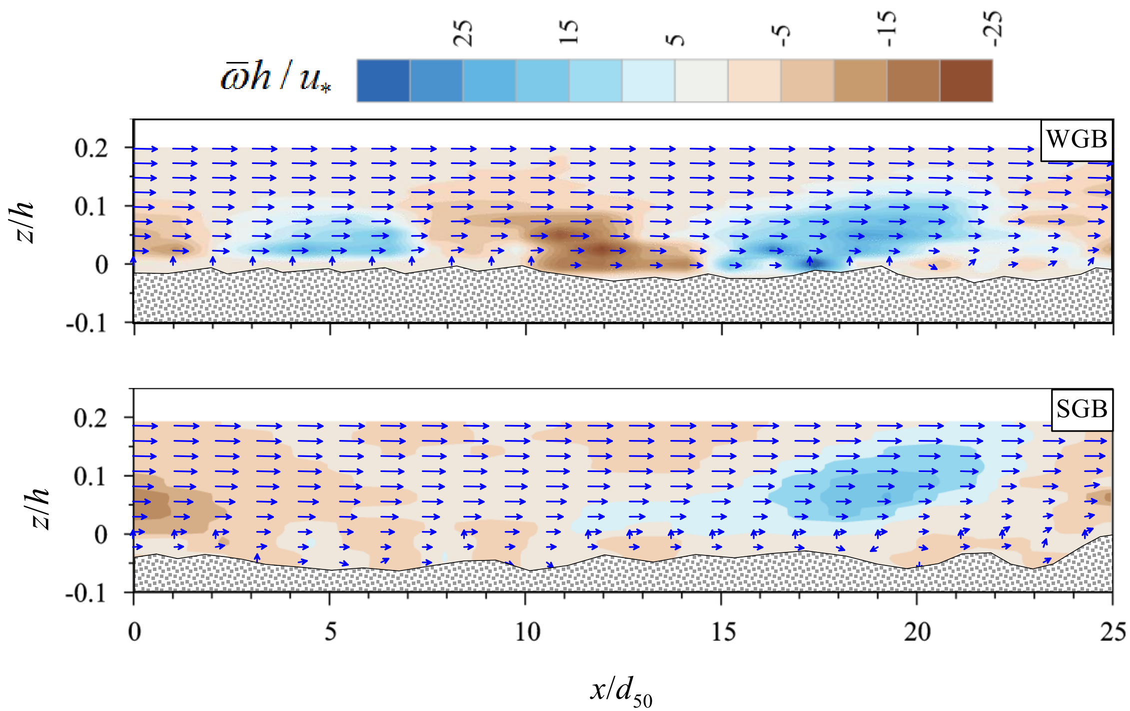

Fig. 5 Time-averaged velocity vectors and vorticity contours $\bar{\omega}\, h/u_*$ on a central vertical plane in the WGB and SGB. The vector → 0.25 (m s^{-1})

Time-averaged streamwise contours and DA streamwise velocity profiles

Time-averaged streamwise velocity is represented as $\bar{u}$ and the DA streamwise velocity is expressed as $\langle \bar{u} \rangle$

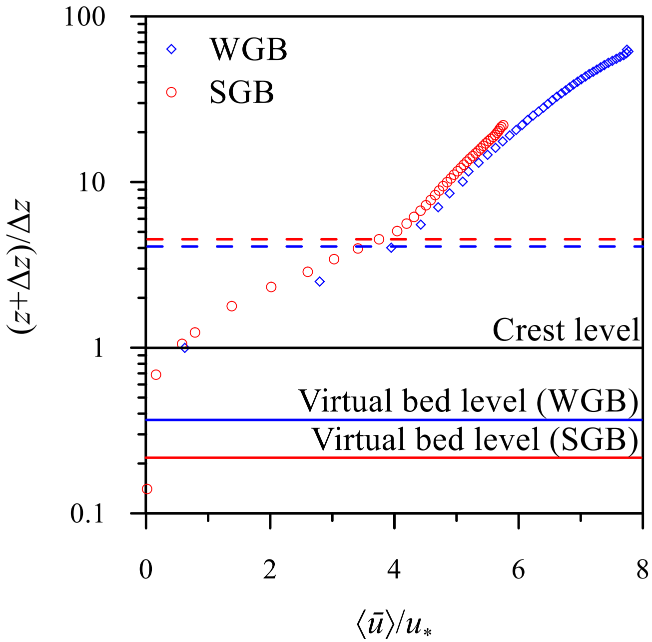

Fig. 7 Variations of DA streamwise velocity $\langle \bar{u} \rangle / u_*$ with $(z+\Delta z)/\Delta z$ in the WGB and SGB

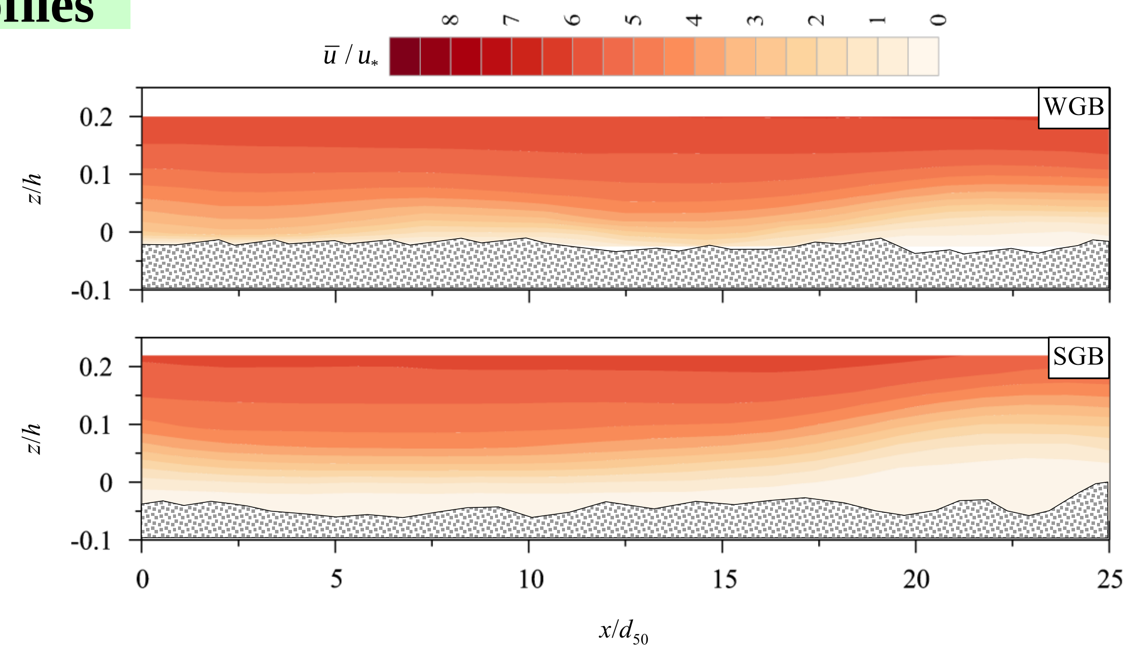

Fig. 6. Contours of dimensionless time-averaged streamwise velocity on a vertical central plane in the WGB and SGB

Here, Δz is the distance of the virtual bed level from the roughness crest

$z_1 = 0$ and $z = \Delta z$ at the virtual bed level

Δz = 2.12 and 4.443 mm from the gravel crest for the WGB and SGB, respectively

RSS contours and spatially averaged (SA) RSS profiles

Reynolds shear stress (RSS) is represented as $-\overline{u'w'}$
and the spatially averaged (SA) RSS is expressed as $\langle -\overline{u'w'} \rangle$

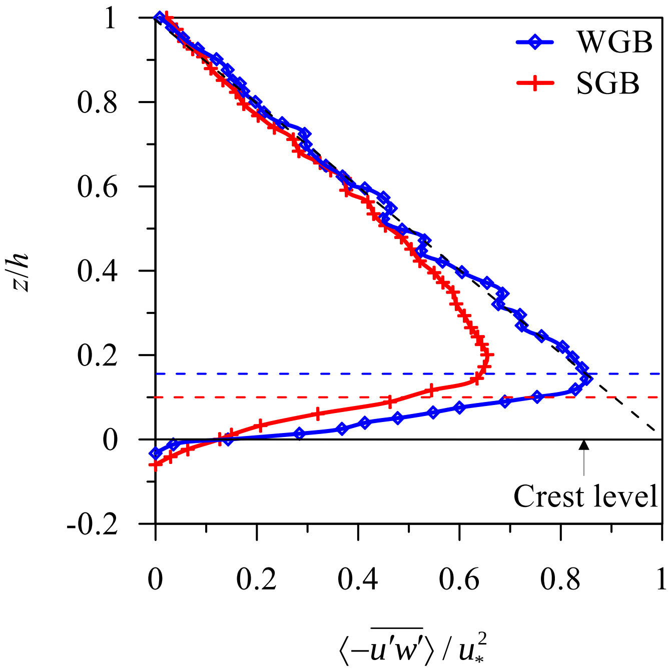

Fig. 9. Variations of SA RSS with z/h in the WGB and SGB

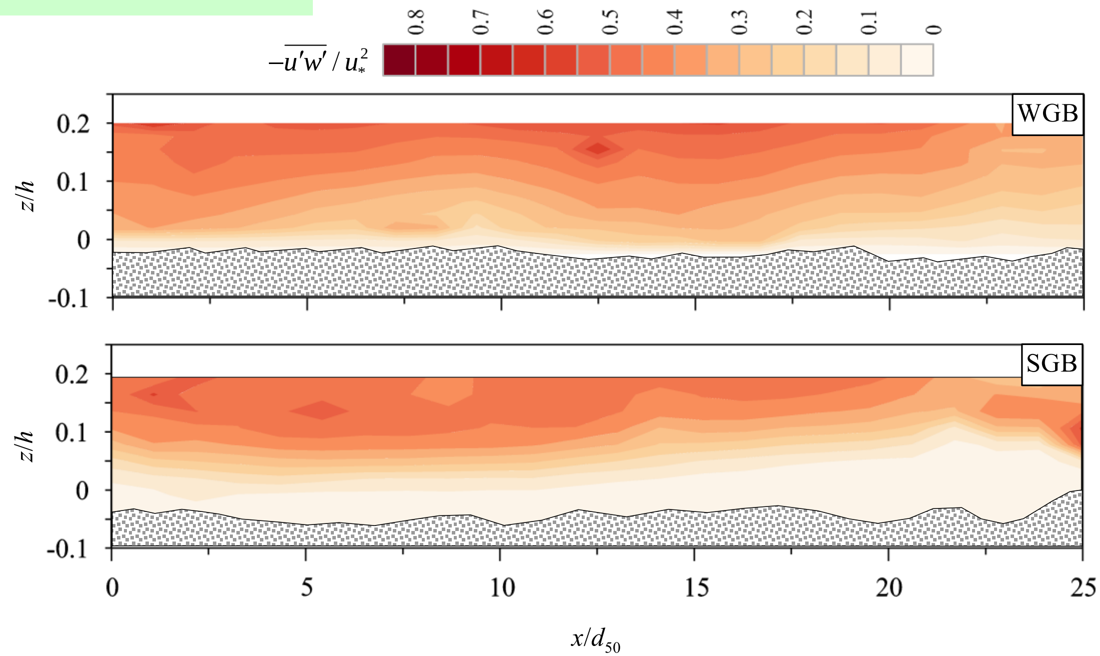

Fig. 8. Contours of dimensionless RSS on a vertical central plane in the WGB and SGB

where u' and w' are the temporal velocity fluctuations in the streamwise and vertical directions, respectively

Total SA shear stress $\tau = \langle -\overline{u'w'} \rangle + \langle -\tilde{u}\tilde{w} \rangle + \langle \tau_v \rangle$

Dispersive shear stress contours and SA dispersive shear stress profiles

SA dispersive shear stress is represented as $\langle -\tilde{u}\tilde{w} \rangle$

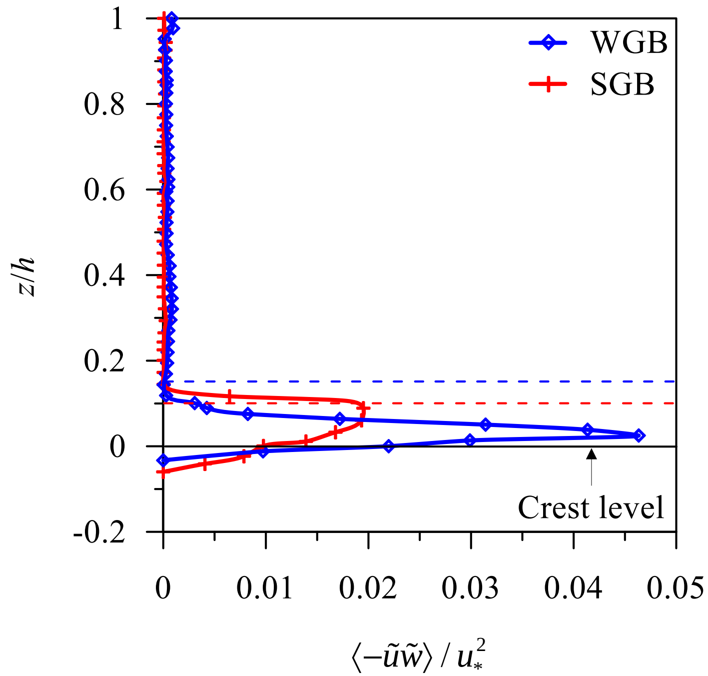

Fig. 11. Variations of SA dispersive shear stress with *z*/*h* in the WGB and SGB

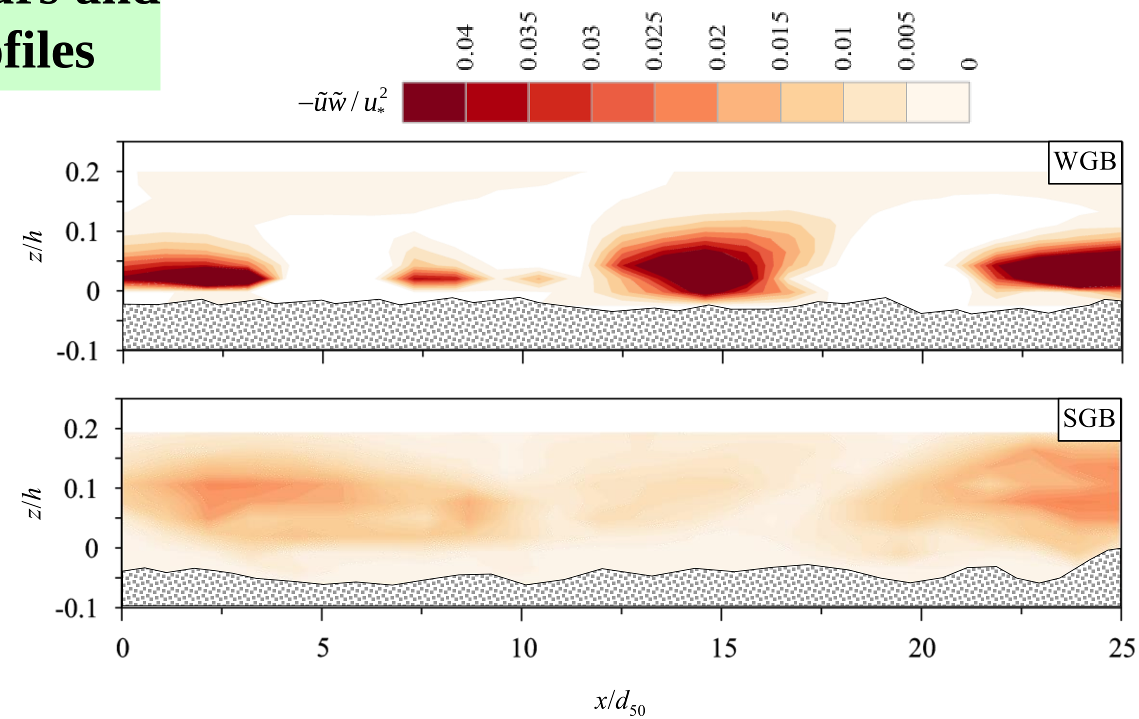

Fig. 10. Contours of dimensionless dispersive shear stress on a vertical central plane in the WGB and SGB

where $\tilde{u}$ and $\tilde{w}$ are the temporal velocity fluctuations in the streamwise and vertical directions, respectively

Contours of TKE streamwise and vertical fluxes

The streamwise TKE flux f_{ku} is estimated as

$$f_{ku} = 0.75(\overline{u'u'u'} + \overline{u'u'w'})$$

and the vertical TKE flux f_{kw} is estimated as

$$f_{kw} = 0.75(\overline{u'w'w'} + \overline{w'w'w'})$$

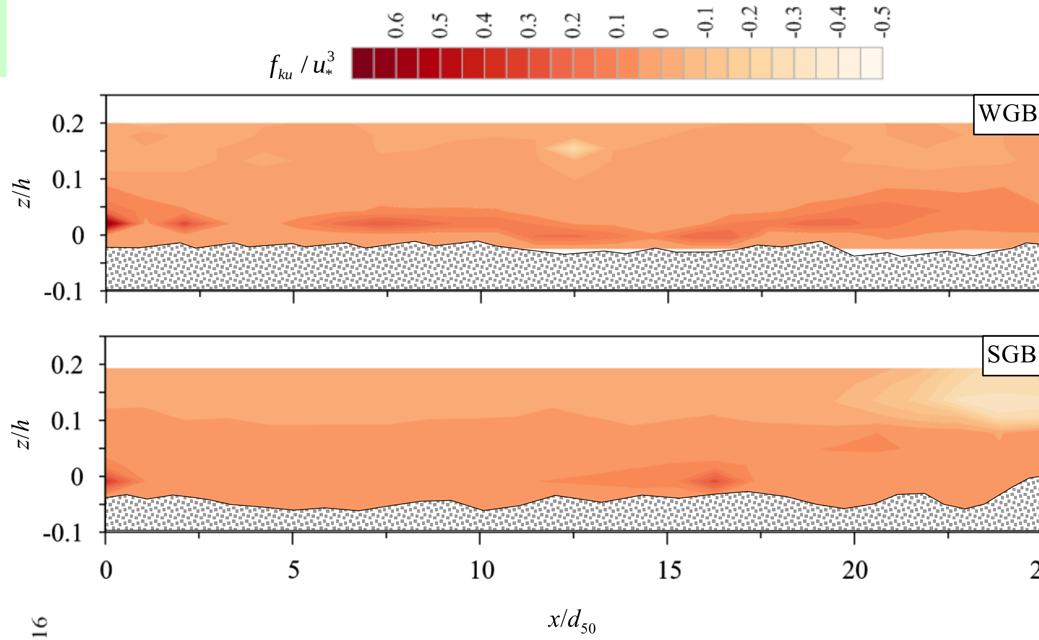

Fig. 12. Contours of dimensionless TKE streamwise flux on a vertical central plane in the WGB and SGB

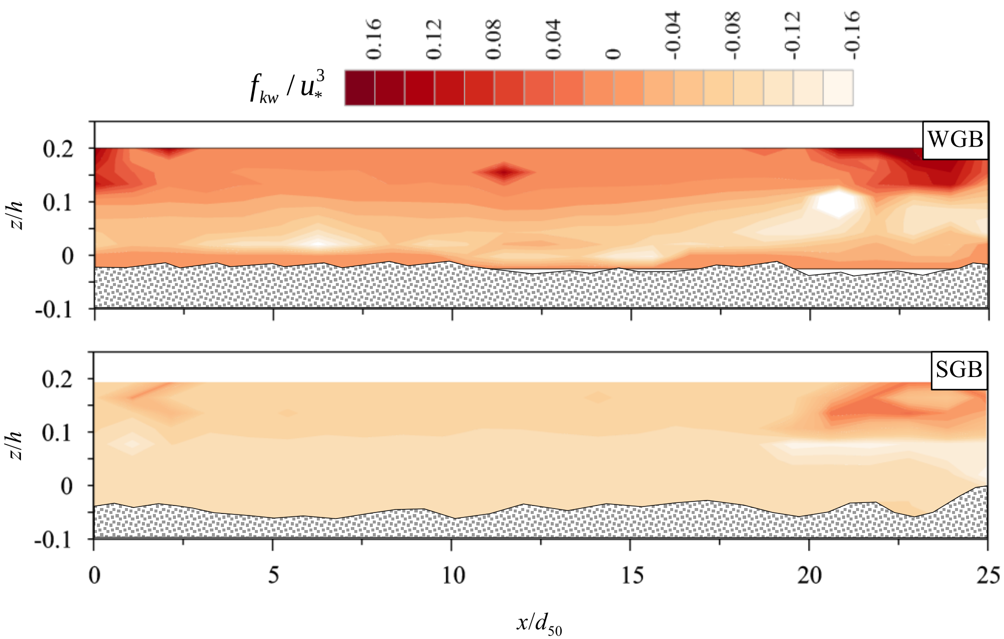

Fig. 13. Contours of dimensionless TKE vertical flux on a vertical central plane in the WGB and SGB

Profiles of SA TKE fluxes and dispersive fluxes

The SA streamwise and vertical TKE fluxes are denoted by $\langle f_{ku} \rangle$ and $\langle f_{kw} \rangle$, respectively, whereas the SA streamwise and vertical dispersive fluxes are as $\langle f_{fu} \rangle$ and $\langle f_{fw} \rangle$ respectively

Here, $\langle f_{fu} \rangle = 0.75(\langle \tilde{u}\tilde{u}\tilde{u} \rangle + \langle \tilde{u}\tilde{u}\tilde{w} \rangle)$ and $\langle f_{fw} \rangle = 0.75(\langle \tilde{u}\tilde{w}\tilde{w} \rangle + \langle \tilde{w}\tilde{w}\tilde{w} \rangle)$

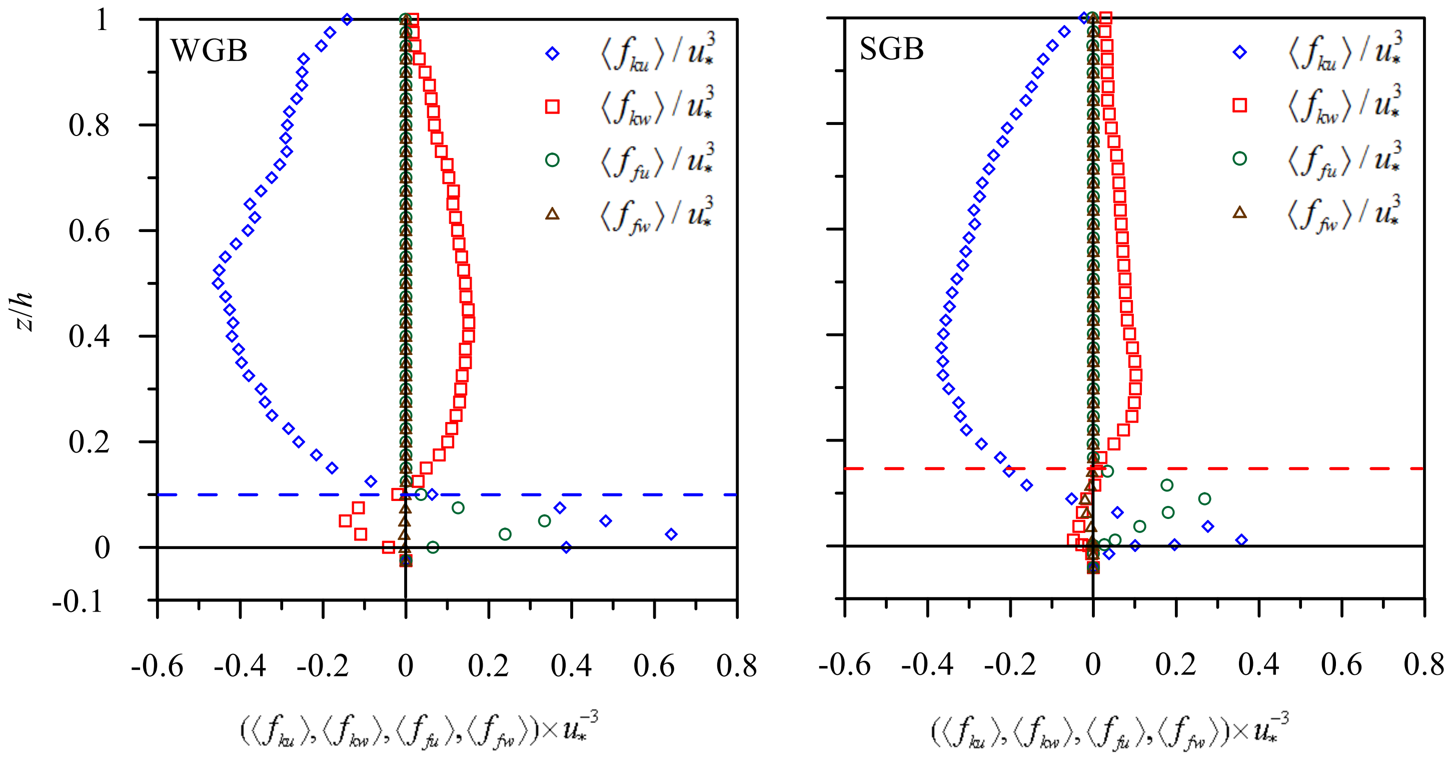

Fig. 14. Variations of SA streamwise TKE flux $\langle f_{ku} \rangle / u_*^3$, SA vertical TKE flux $\langle f_{kw} \rangle / u_*^3$, dispersive streamwise TKE flux $\langle f_{fu} \rangle / u_*^3$, and dispersive vertical TKE flux $\langle f_{fw} \rangle / u_*^3$ with z/h in the WGB and SGB

SA turbulent kinetic energy (TKE) budget equation

$$\underbrace{-\langle\overline{u'w'}\rangle\frac{\partial\langle\bar{u}\rangle}{\partial z}}_{\substack{\text{TKE production rate}\\(t_P)}} = \underbrace{\langle\varepsilon\rangle}_{\text{TKE dissipation rate}} + \underbrace{\frac{\partial\langle f_{kw}\rangle}{\partial z}}_{\substack{\text{TKE diffusion rate}\\(t_D)}} + \underbrace{\frac{1}{\rho}\frac{\partial\langle\overline{p'w'}\rangle}{\partial z}}_{\substack{\text{Pressure energy diffusion rate}\\(p_D)}} - \underbrace{\nu\frac{\partial^2\langle k\rangle}{\partial z^2}}_{\substack{\text{Viscous diffusion rate}\\(\nu_D)}}$$

Here ρ is the mass density of water

According to Kolmogorov's second hypothesis, within the inertial subrange, the dissipation rate ε can be estimated using second order velocity structure function, such that

$$\varepsilon = \frac{1}{r}\left(\frac{\Delta u^2}{C_2}\right)^{3/2}$$

where Δu is the streamwise velocity increment along the spatial distance in the streamwise direction, expressed as $\Delta u = \langle[u'(x+r)-u'(x)]\rangle$, C_2 is a universal constant equaling 2.12, x is the measuring distance in the streamwise direction from a convenient location, r is the separation distance between two measuring locations

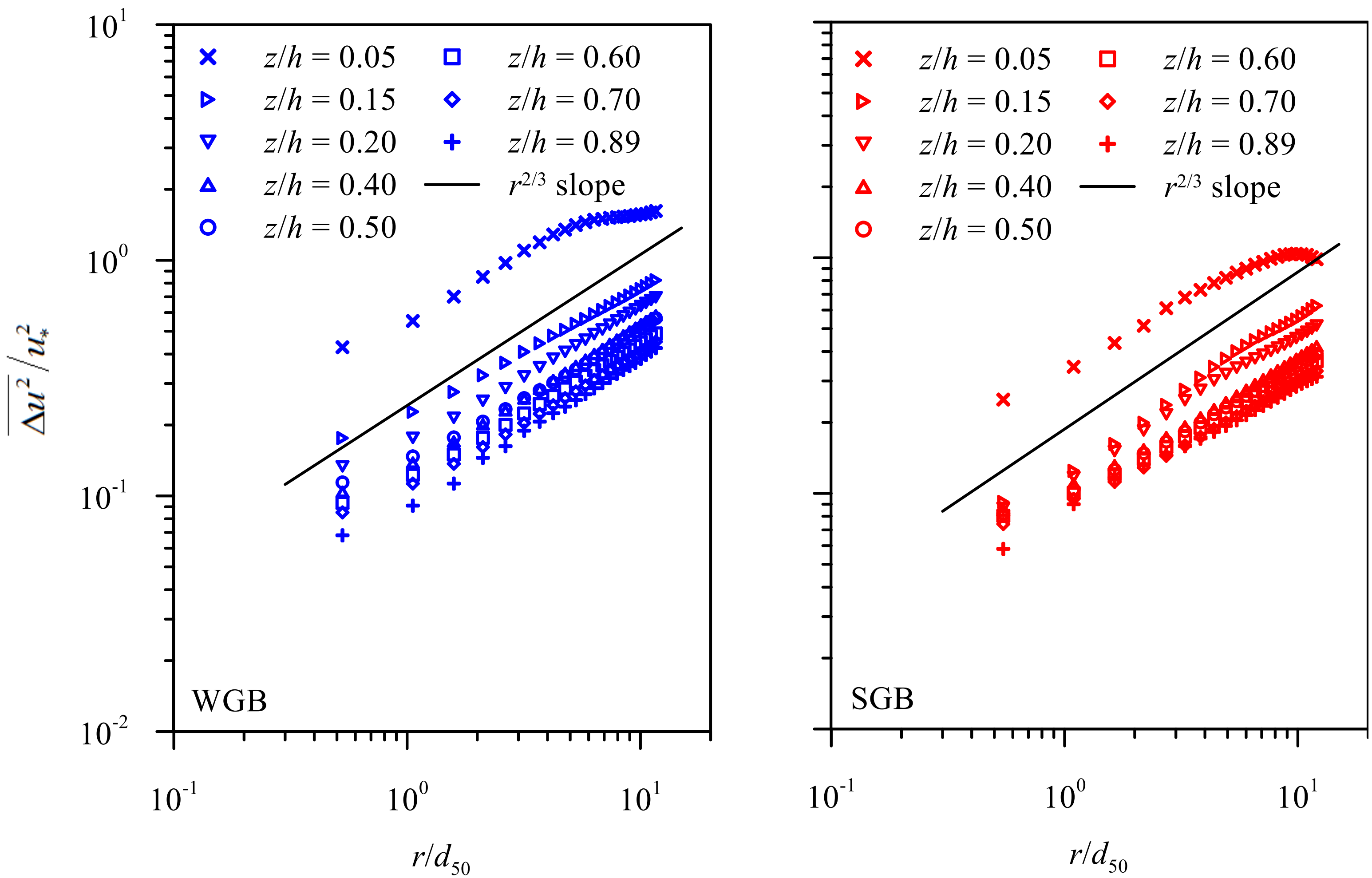

Fig. 15. Variations of second-order velocity structure function $\overline{\Delta u^2}/u_*^2$ with r/d_{50} for different z/h in the WGB and SGB

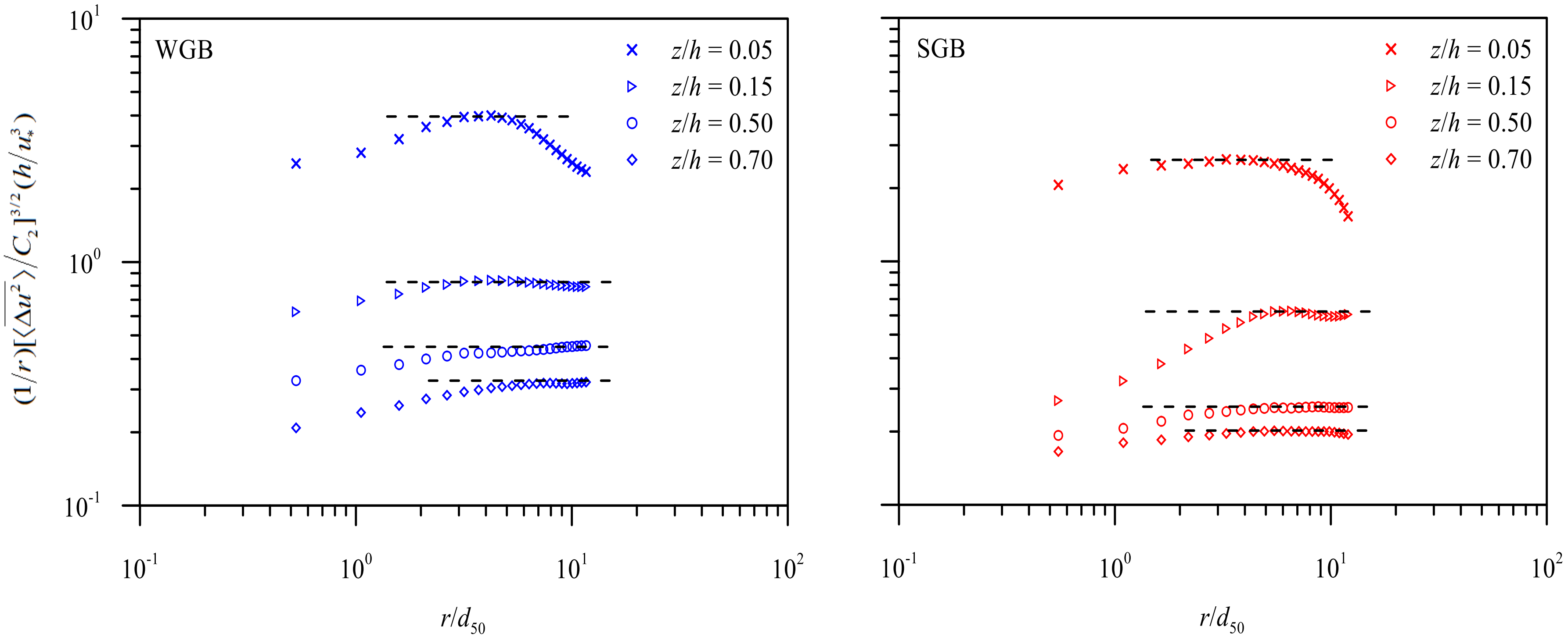

Fig. 16. Variations of Kolmogorov's SA two-thirds law with r/d_{50} for different z/h in the WGB and SGB

TKE production rate contours and SA TKE production rate profiles

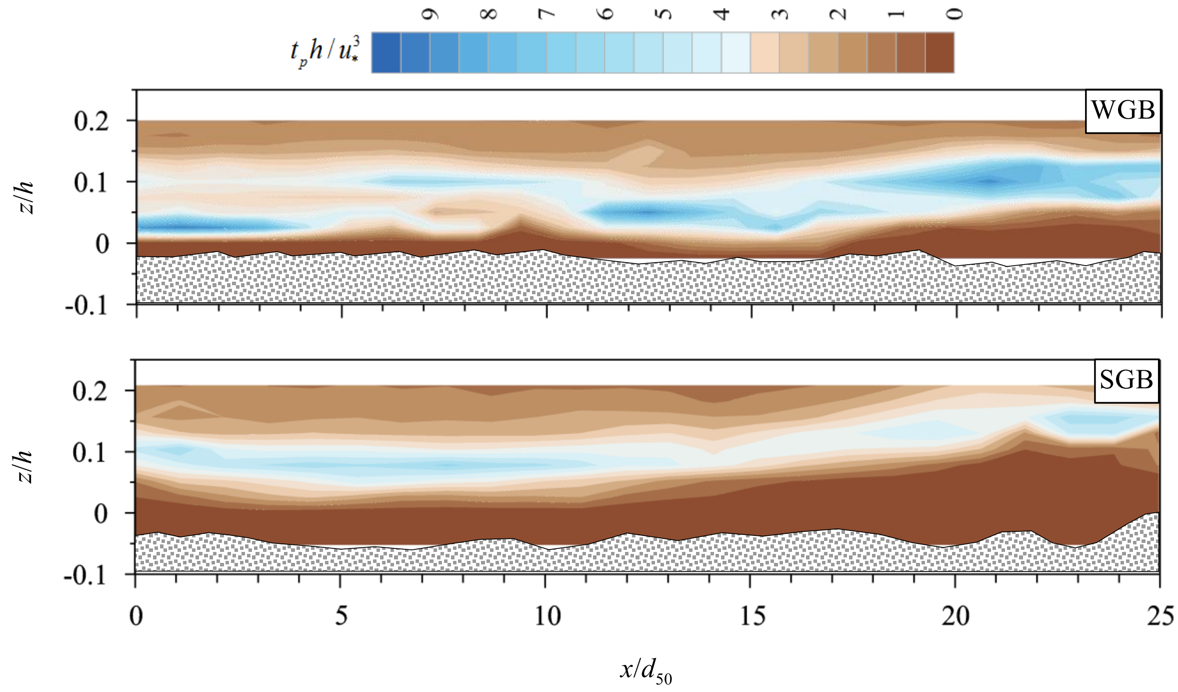

Fig. 17. Contours of dimensionless TKE production rate on a vertical central plane in the WGB and SGB

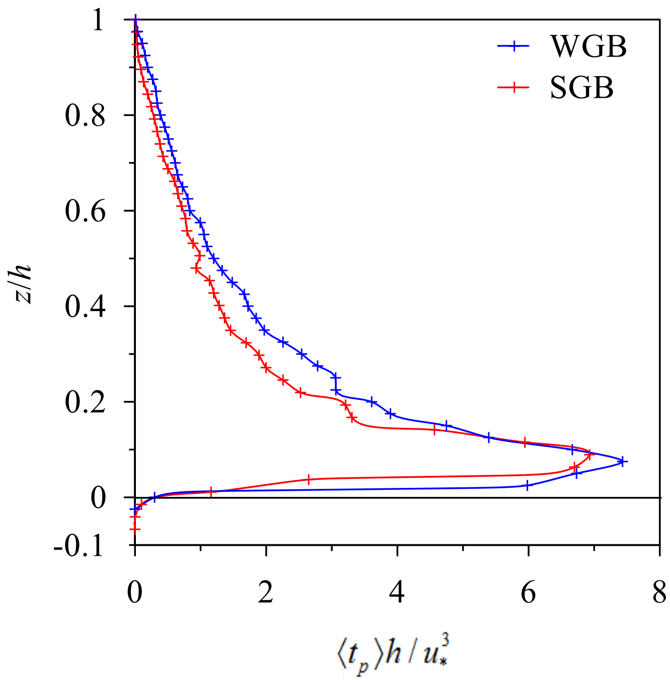

Fig. 18. Variations of dimensionless SA TKE production rate with z/h in the WGB and SGB

TKE dissipation rate contours and SA TKE dissipation rate profiles

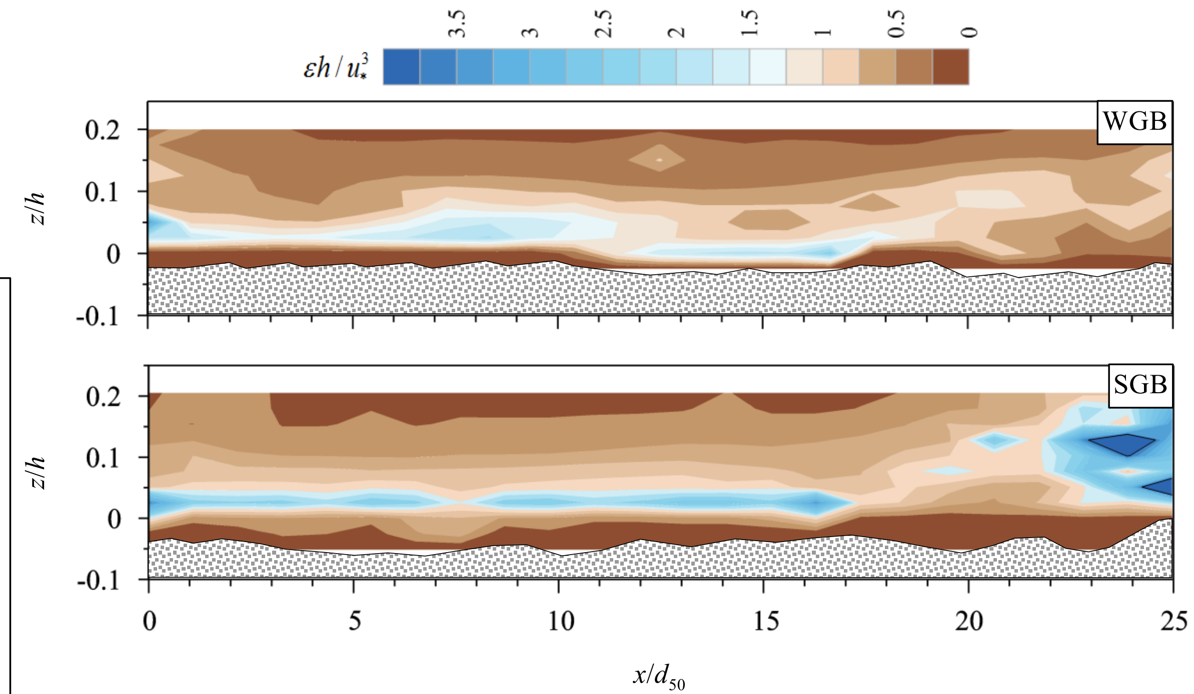

Fig. 19. Contours of dimensionless TKE dissipation rate on a vertical central plane in the WGB and SGB

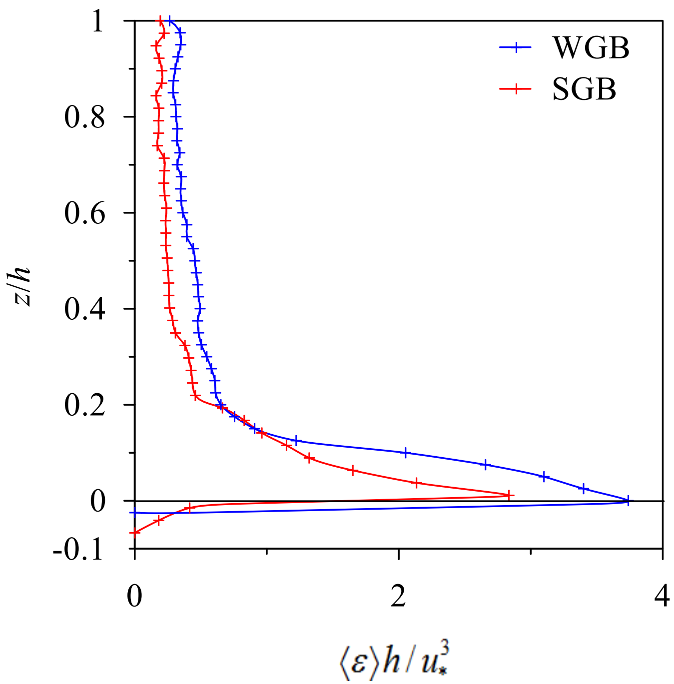

Fig. 20. Variations of dimensionless SA TKE dissipation rate with *z*/*h* in the WGB and SGB

TKE diffusion rate contours and SA TKE diffusion rate profiles

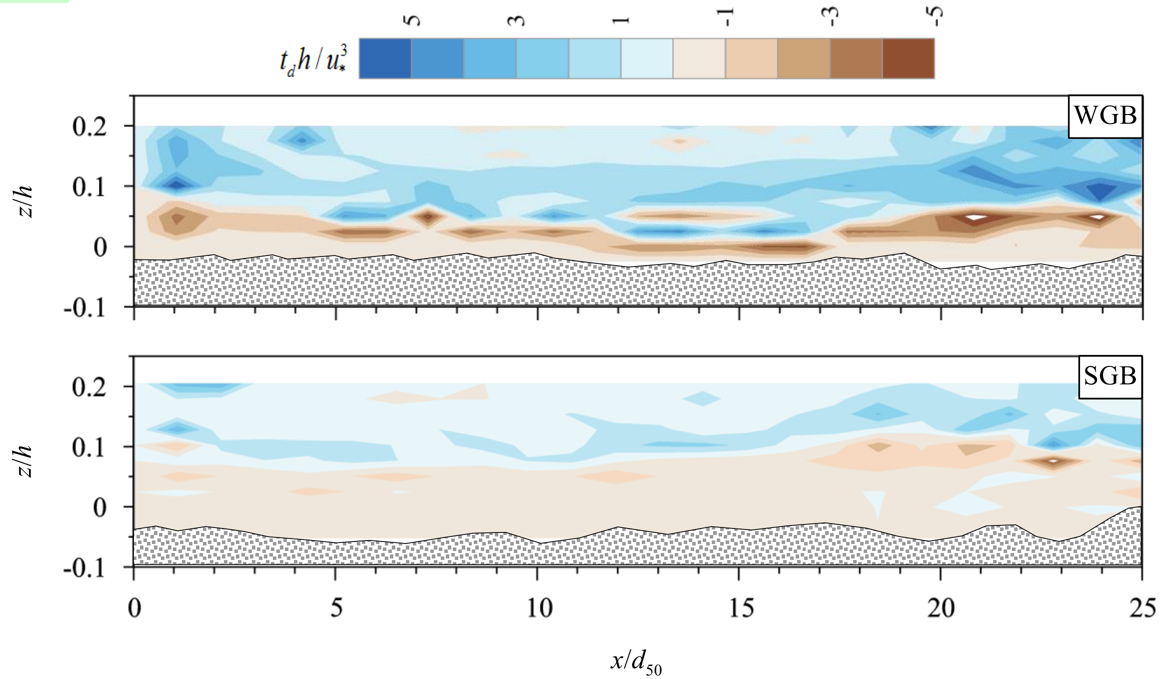

Fig. 21. Contours of dimensionless time-averaged TKE diffusion rate on a vertical central plane in the WGB and SGB

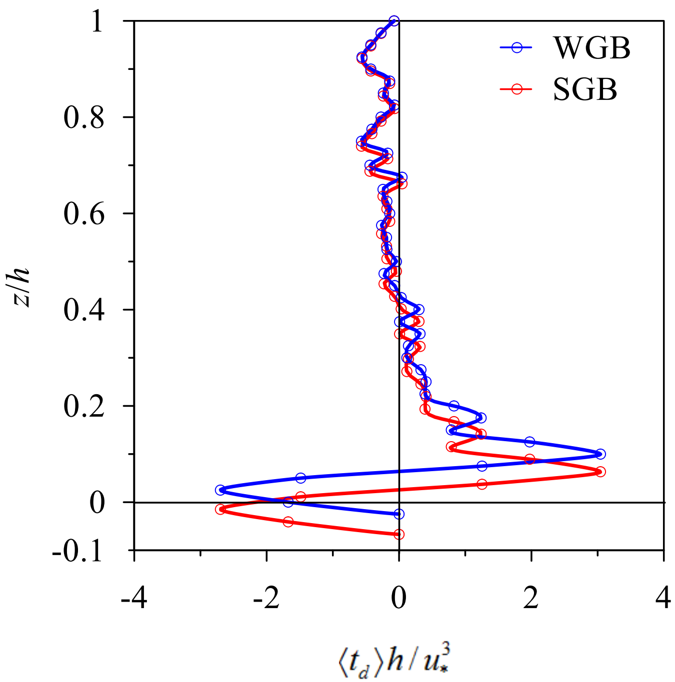

Fig. 22. Variations of dimensionless SA TKE diffusion rate with z/h in the WGB and SGB

Pressure energy diffusion rate contours and SA pressure energy diffusion rate profiles

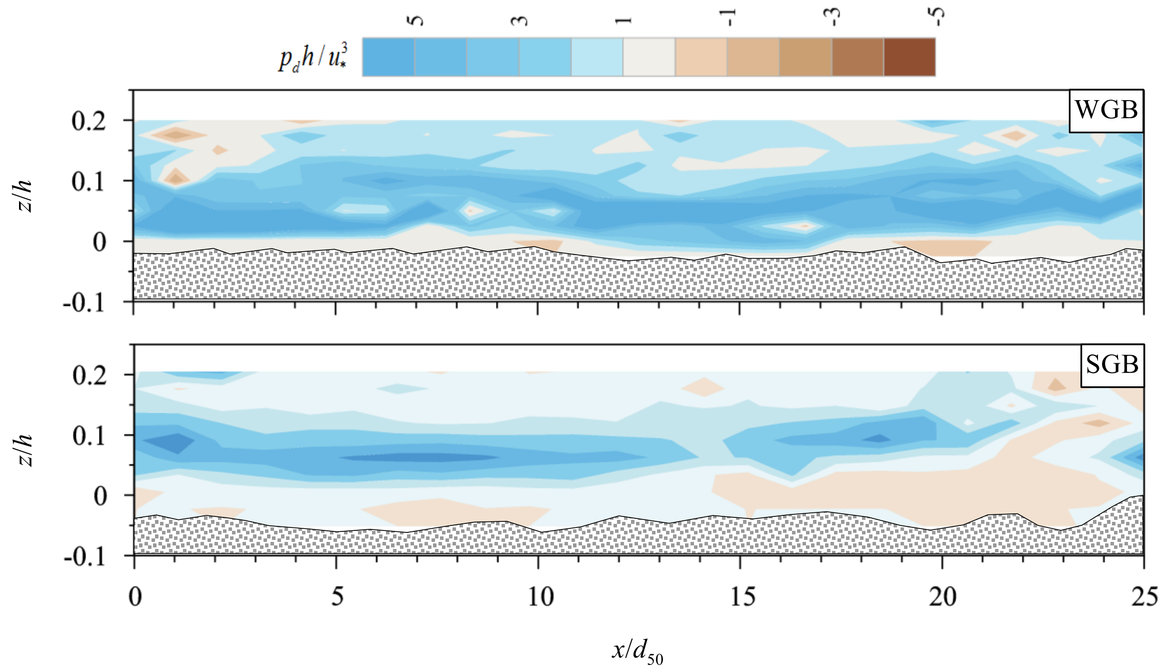

Fig. 23. Contours of dimensionless pressure energy diffusion rate on a vertical central plane in the WGB and SGB

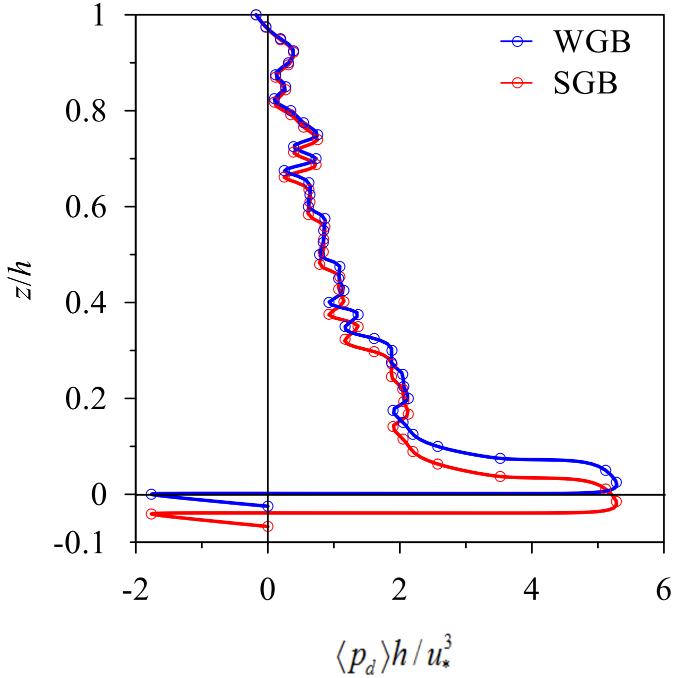

Fig. 24. Variations of dimensionless SA pressure energy diffusion rate with z/h in the WGB and SGB

Conclusions

- Action of water work changes the randomly poised SGB roughness structure to the organized WGB roughness structure with a higher roughness
- At a given vertical distance, all the turbulence parameters are observed to be higher in WGB than those in the SGB
- The SA TKE flux plots reveals that the sweeps are the governing events in the near-bed flow zone, while in the main flow, the ejections dominate
- For small values of separation distance, the second-order velocity structure function follows the 2/3 slope, indicating the presence of inertial subrange in both the beds

Recommendation

As it is seen that SGB underestimates the turbulence characteristics, therefore it is prudent to perform experimental study in a WGB, while the results obtained from SGB should be used with precaution.

Thank you